

Design and Feasibility Assessment of Transport Operations for Delivering Typhoon Control Substances

Hiroki Akiyama[1], Seiya Ueno[1], Takehiro Higuchi[1] & Tomohiro Sakurai[1]
[1] Institute for Multidisciplinary Sciences, Yokohama National University

Abstract

Controlling tropical cyclone impacts is a critical global challenge addressed by Japan's Moonshot Research and Development Program, Goal 8[1]. This study develops a numerical simulation framework comprising four operational modes to evaluate the feasibility of substance delivery for typhoon control, using seven candidate airfields and two historical typhoon trajectories. Airfield selection was based strictly on runway infrastructure and geographic distribution. A supplementary geographic sensitivity study examines two actual Japanese remote Pacific island locations—Minamitorishima and Okinotorishima—assuming the availability of airfields with takeoff and landing capability, to quantify the upper bound of geographic advantage. Results demonstrate that track alignment governs operational throughput; campaign window duration—not sortie frequency—is the primary differentiator for high-speed delivery platforms; and maritime platforms require advance Pacific pre-positioning to achieve meaningful delivery rates.

Keywords: Typhoon Control, Transport Operations, Feasibility Assessment

1. Introduction

The increasing frequency and intensity of tropical cyclones pose a critical threat to global society. Typhoons making landfall in the Asia-Pacific region cause enormous economic damage every year and at times result in significant loss of life. Japan's Moonshot Research and Development Program, Goal 8[1], represents a major initiative to develop typhoon control technologies capable of reducing these impacts by directly modifying the thermodynamic structure of approaching typhoons.

Any effective typhoon intervention requires both: (1) the bulk aerial delivery of influence substances—hygroscopic aerosols, ice-nucleating particles, or other thermodynamically active materials—into the storm system using transport aircraft (Modes 1-3); and (2) the rapid precision delivery of concentrated influence packages by high-speed aerial platforms and maritime surface vessels (Mode 4). While the logistical feasibility of transport operations remains largely understudied prior vehicle routing formulations [6–10] have addressed multi-vehicle dispatch optimization but have not been applied to the typhoon delivery context, the high-speed delivery dimension presents additional operational challenges related to platform speed, operational geometry, and sortie tempo. This paper addresses both dimensions through a unified simulation framework.

Seven candidate airfields were selected based solely on infrastructure suitability and geographic distribution, with no implication of specific organizational involvement. A supplementary sensitivity analysis in Section 5 further quantifies the geographic upper bound using two actual Japanese remote Pacific island locations—Minamitorishima and Okinotorishima—assuming the availability of airfields with takeoff and landing capability at each site.

2. Simulation Framework

2.1 Typhoon Data Model

Two historical typhoon trajectories provide contrasting geometric test cases. Typhoon Meari (2004)

followed a recurving track from the central Pacific, executing a right-hand turn near 20°N before traversing southwestern Japan. Typhoon Vera (1959) followed a direct southwest-to-northeast track, making a devastating landfall at Ise Bay. Position data (latitude, longitude, central pressure) were obtained from the Japan Meteorological Agency best-track dataset at 6-hour intervals with linear interpolation applied at each simulation time step.

2.2 Strong Wind Radius and Operational Termination

The strong wind radius $R15$—the radius within which sustained surface wind exceeds 15 m/s—defines the operational exclusion zone. $R15$ is estimated from the typhoon central pressure P (hPa) at each time step:

$$R15 = max(100,\ (1013 - P) \times 5) \quad [km]$$

Here, $(1013 - P)$ represents the central pressure deficit from standard sea-level pressure (1013 hPa), which serves as a proxy for typhoon intensity. A larger pressure deficit corresponds to a stronger and more radially extensive wind field, yielding a proportionally larger R15. The lower bound of 100 km ensures a physically meaningful minimum strong wind radius even for weak systems.

Operations terminate when the strong wind zone ($R15$) reaches the airfield—that is, when the distance from the typhoon center to the airfield falls to or below $R15$. An additional safety buffer $D_safe = 400$ km is also enforced. Aircraft in sortie when either condition is triggered complete their return before operations cease.

2.3 Platform Performance Models

The simulation models two classes of platforms. Modes 1-3 use bulk transport aircraft (Table 1). Mode 4 uses high-speed aerial delivery platforms (cruise speed 890 km/h, operational range 4,500 km, delivering 4 packages per sortie) and maritime surface platforms (cruise speed 37 km/h, operational radius 250 km, delivering 8 packages per delivery operation). The operational definitions and design rationale for each mode are described in Section 2.5.

Table 1 - Transport aircraft parameters (Modes 1-3) [2][3][4][5].

Aircraft Model	Category	Speed (km/h)	Range (km)	Payload (t)
Kawasaki C-2 (Long-Range)	Long-Range Jet	890	7,600	20
Kawasaki C-2 (High-Capacity)		890	4,500	36
C-130H Hercules	Tactical Turboprop	550	3,800	19
Q400AT	Civil Turboprop	660	2,440	14
MQ-9 Reaper (UAV)	Unmanned Aerial Vehicle	300	5,000	1.7

2.4 Airfield Selection

Seven candidate departure airfields were selected based on runway length >= 2,500 m and geographic distribution across latitudes. Selection represents purely geographic and infrastructure constraints without organizational implications.

Table 2 - Candidate departure airfields.

Airfield	Pref.	Lat. (°N)	Lon. (°E)
Iruma Air Base	Saitama	35.84	139.41
Komaki Air Base	Aichi	35.25	136.92
Kansai Intl. Airport	Osaka	34.43	135.23
Miho Air Base	Tottori	35.49	133.24
Tsuiki Air Base	Fukuoka	33.68	131.05
Kagoshima Airport	Kagoshima	31.80	130.72
Naha Airport	Okinawa	26.20	127.65

Table 3 - Candidate maritime departure ports.

Port	Prefecture	Lat. (°N)	Lon. (°E)
Yokosuka Naval Base	Kanagawa	35.28	139.68
Maizuru Naval Base	Kyoto	35.47	135.38
Kure Naval Base	Hiroshima	34.23	132.57
Sasebo Naval Base	Nagasaki	33.17	129.72
Ominato Naval Base	Aomori	41.08	141.25

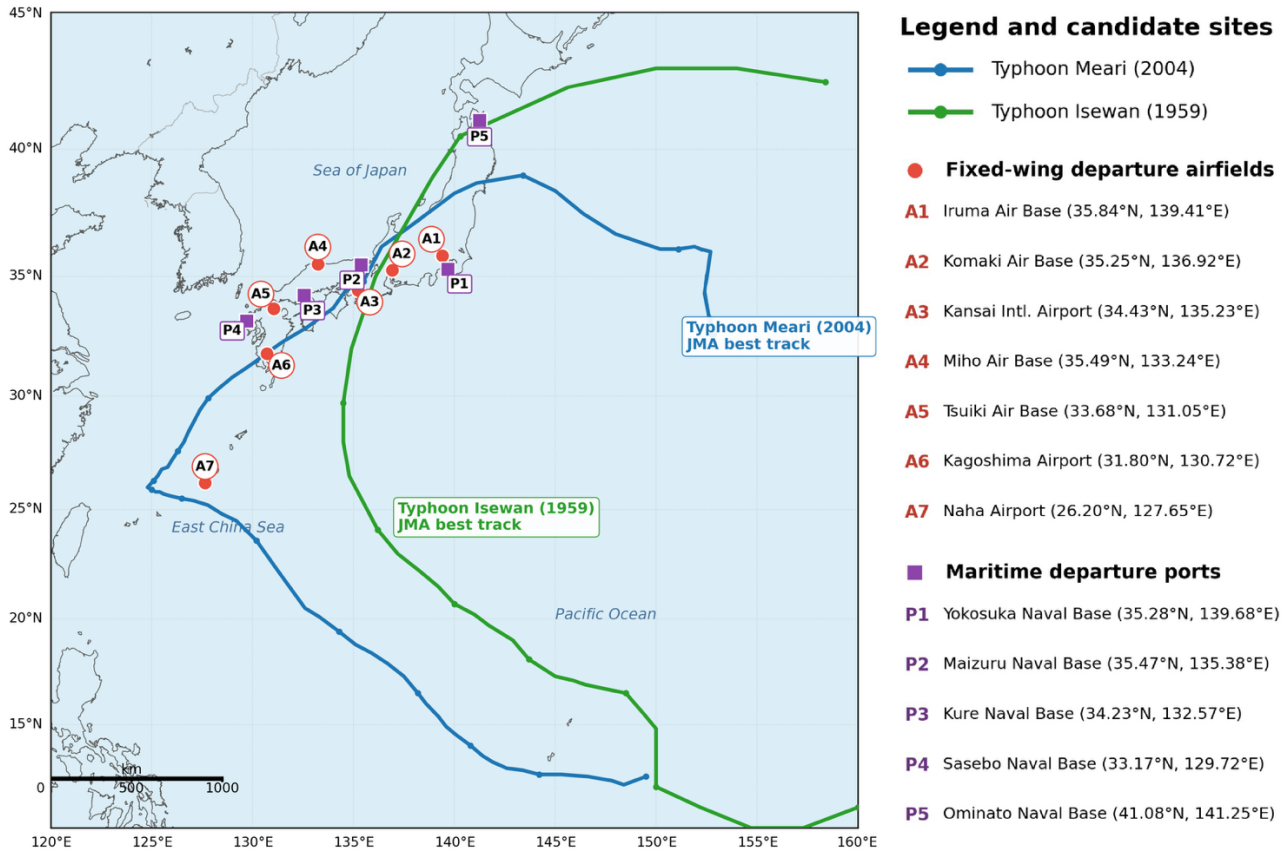


Figure 1 - Typhoon tracks (Typhoon Meari (2004), Typhoon Vera (1959)) and candidate departure airfields.

2.5 Simulation Modes

Four simulation modes evaluate distinct operational dimensions. All modes apply the R15 and D_safe termination conditions described in Section 2.2.

- **Mode 1 (Fixed Fleet)**: Continuous rotation of one aircraft per type; measures total sorties and cumulative transport volume. This mode was designed to evaluate the effect of airfield geography on transport throughput, by holding fleet size constant at one aircraft per type.

- **Mode 2 (Fixed Lap)**: Evaluates completion of N = 1, 2, or 3 circumnavigation laps around the typhoon core (~50 km radius) within a single sortie fuel budget. This mode was designed to evaluate which aircraft–airfield combinations can support multi-pass seeding missions within a single sortie fuel budget.

- **Mode 3 (Fuel Limit)**: Allows on-station loitering until fuel reaches minimum safety reserve (return + 10%), measuring maximum laps per sortie. This mode was designed to evaluate the upper bound on on-station seeding intensity per sortie, quantifying maximum cumulative seeding exposure per platform before reaching minimum fuel reserve.

- **Mode 4 (Precision Delivery)**: Evaluates high-speed aerial delivery platforms (890 km/h, 4,500 km range) and maritime surface platforms (37 km/h, 250 km operational radius). For aerial platforms, one sortie delivers 4 packages; each maritime delivery operation delivers 8 packages. The mode tracks both the number of delivery events and the temporal distribution across the campaign. This mode was designed to evaluate the precision-delivery capability of high-speed aerial and maritime surface platforms, assessing whether these platforms can achieve sufficient delivery frequency and temporal coverage for targeted typhoon zone influence.

3. Results

3.1 Fixed Fleet Mode (Mode 1)

Figures 2-5 show total sortie counts and transport volumes for both typhoon cases. For Typhoon Meari (2004), Naha Airport leads all seven existing airfields with 70 sorties and 1,442 t, driven by activation of the Q400AT and higher C-130H rates. Mainland airfields achieve 45-59 sorties. For Typhoon Vera (1959), the performance ranking reverses: Kagoshima tops the list at 46 sorties (965 t), while Naha drops to 36 sorties (761 t). This track-dependent reversal is the central structural finding across all simulation modes.

Table 4 - Mode 1 summary

Airfield	Typhoon			
	Meari (2004)		Vera (1959)	
	Sorties	Vol. (t)	Sorties	Vol. (t)
Iruma	54	1,184	31	687
Komaki	52	1,128	33	720
Kansai	53	1,147	36	772
Miho	45	975	32	701
Tsuiki	50	1,078	39	824
Kagoshima	59	1,253	46	965
Naha	70	1,442	36	761

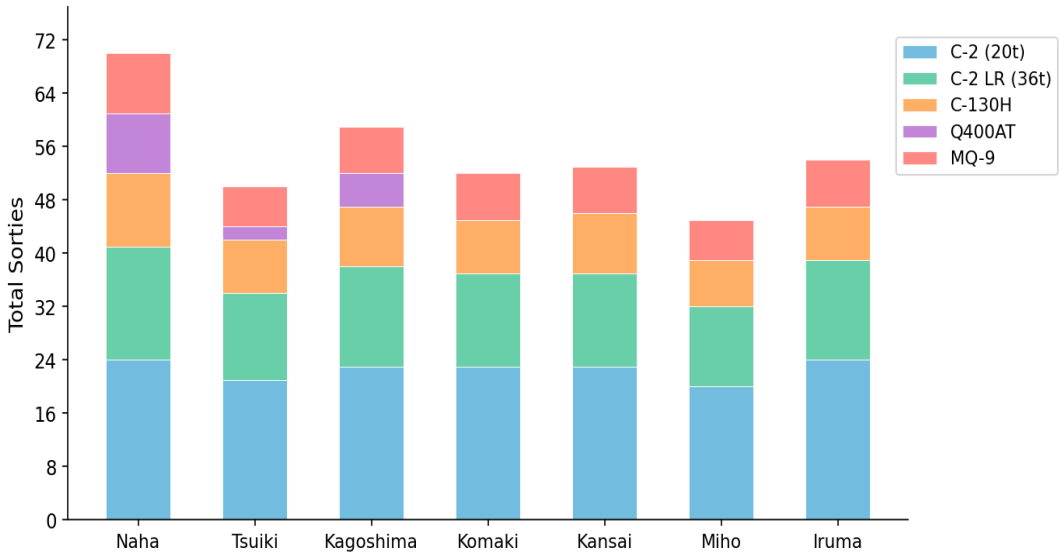


Figure 2 - Mode 1 sortie count (Typhoon Meari (2004)).

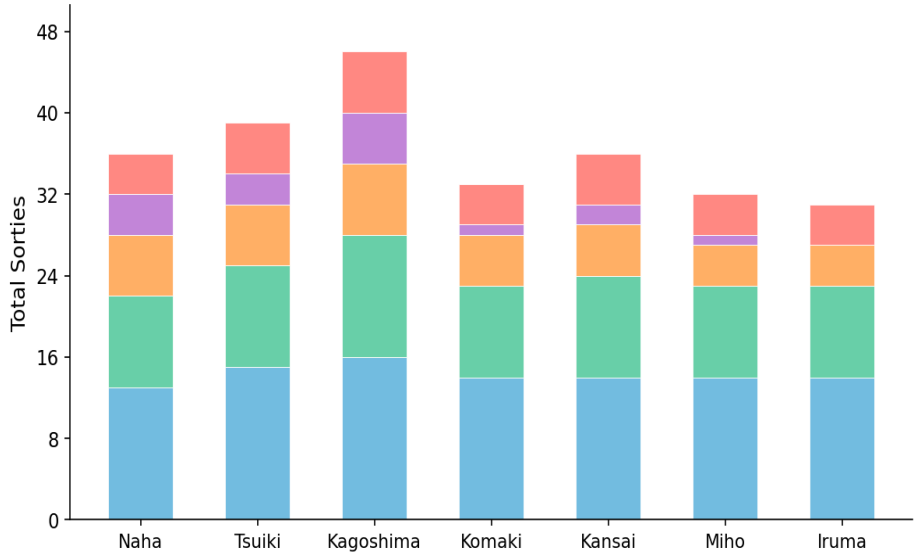


Figure 3 - Mode 1 sortie count (Typhoon Vera (1959)).

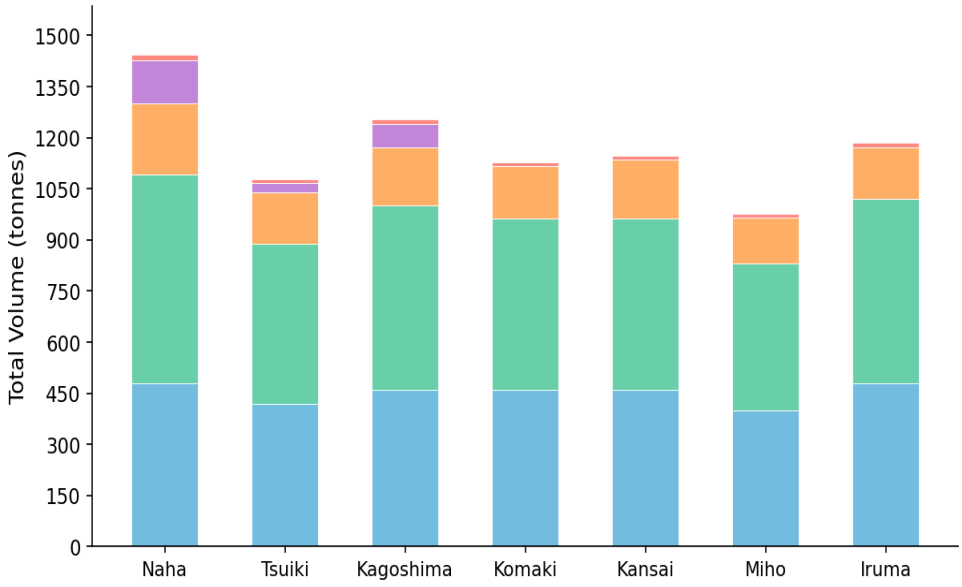


Figure 4 - Mode 1 transport volume (Typhoon Meari (2004)).

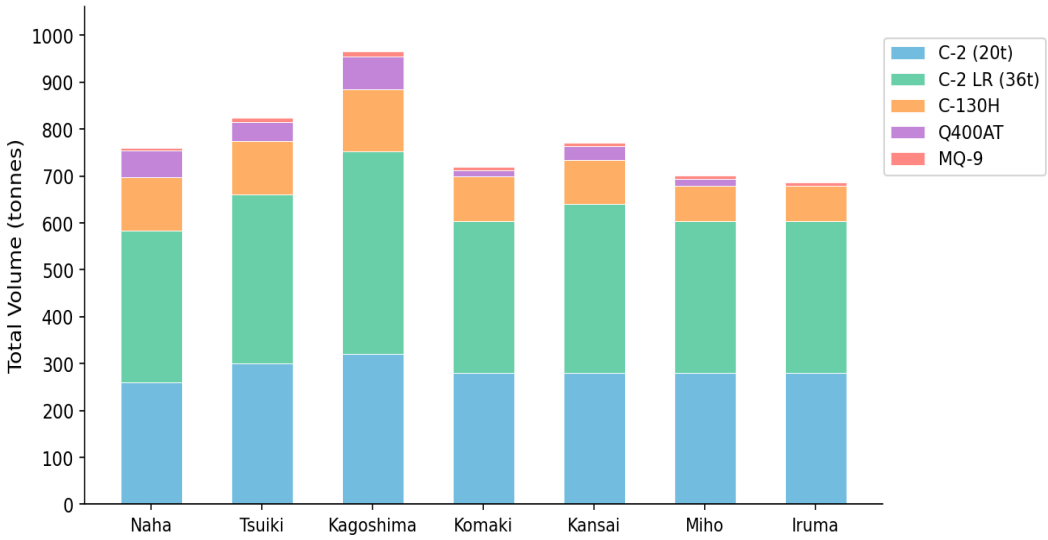


Figure 5 - Mode 1 transport volume (Typhoon Vera (1959)).

3.2 Fixed Lap Mode (Mode 2)

Figure 6 presents qualifying sorties for one-lap, two-lap, and three-lap missions. For single-lap missions, four aircraft types (C-2 Long-Range, C-2 High-Capacity, C-130H, and MQ-9) qualify from all seven airfields, while the Q400AT qualifies only from Naha. For two-lap missions, the C-130H drops out from Iruma, Komaki, Miho, and Kansai; Q400AT remains viable from Naha only. For three-lap missions, only the C-2 Long-Range and MQ-9 maintain coverage from all seven airfields; C-2 High-Capacity qualifies from Naha, Kagoshima, and Tsuiki; C-130H is viable from Naha only; Q400AT achieves no three-lap completions from any airfield.

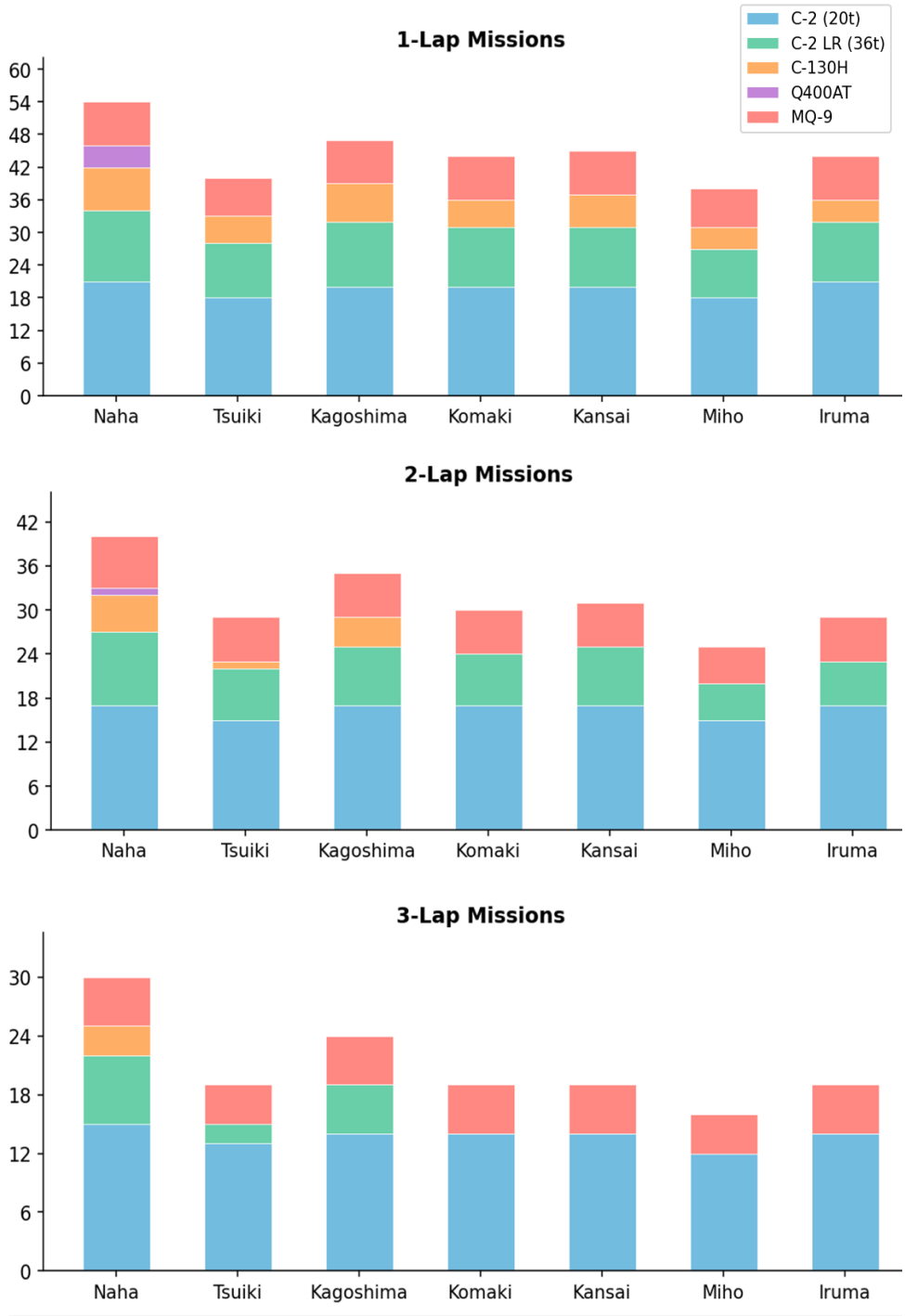


Figure 6 - Mode 2 fixed lap count: qualifying sorties for one-lap (top), two-lap (middle), and three-lap (bottom) missions (Typhoon Meari (2004)).

3.3 Fuel Limit Mode (Mode 3)

Figure 7 shows average maximum laps per sortie. From Naha: C-2 Long-Range averages 5.1 laps, MQ-9 3.9, C-130H 2.2, Q400AT 1.3. From Iruma: C-2 Long-Range 4.5 laps, C-130H 0.9, Q400AT 0 (infeasible). The MQ-9 maintains consistent performance across all locations, confirming its role as a location-independent persistence platform.

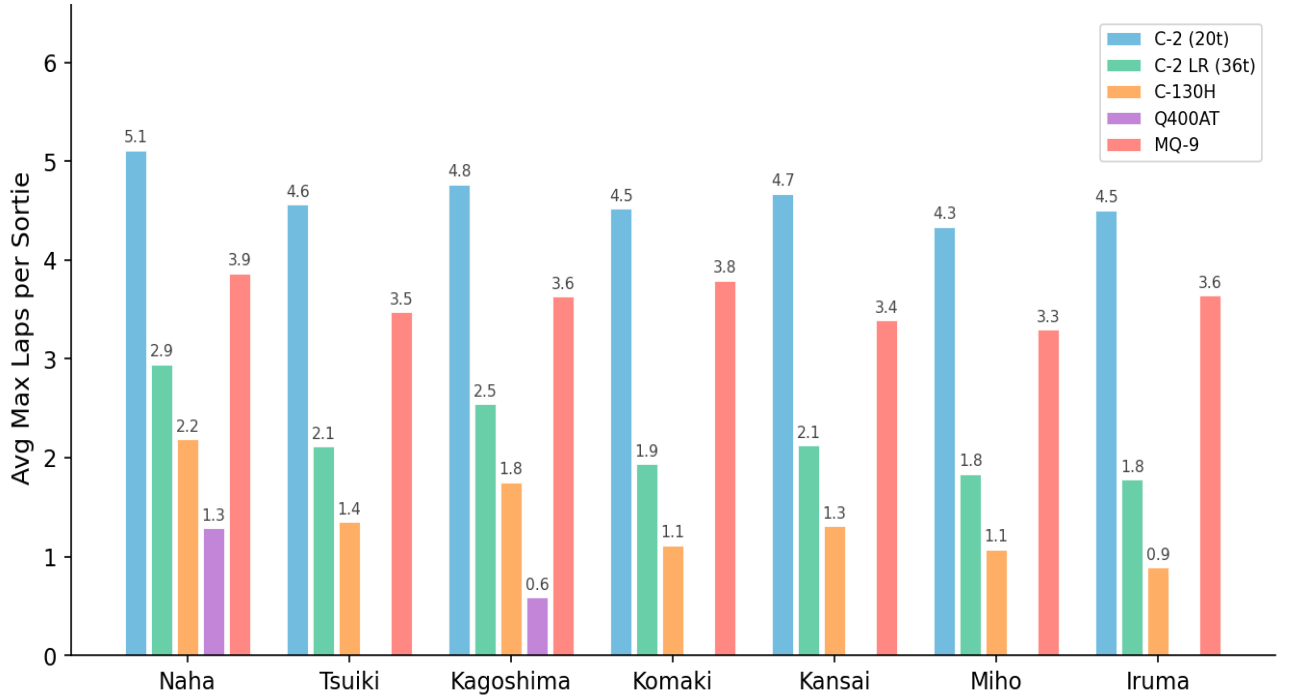


Figure 7 - Mode 3 average maximum laps per sortie (Typhoon Meari (2004)).

3.4 Delivery Mode (Mode 4)

Mode 4 evaluates high-speed aerial delivery platforms and maritime surface platforms. The sea position analysis is shown in Figure 1. Figures 8, 9, and 10 show detailed quantitative results for Mode 4.

3.4.1 Mode 4 — Aerial Delivery Platform Results

Figure 8 presents the full delivery event timeline for the Typhoon Meari (2004) campaign. Each dot represents one delivery sortie; its horizontal position gives the timing. A striking pattern emerges: despite the large range differences between airfields that strongly differentiated Modes 1-3, the aerial delivery platforms show remarkably consistent performance across all seven existing locations.

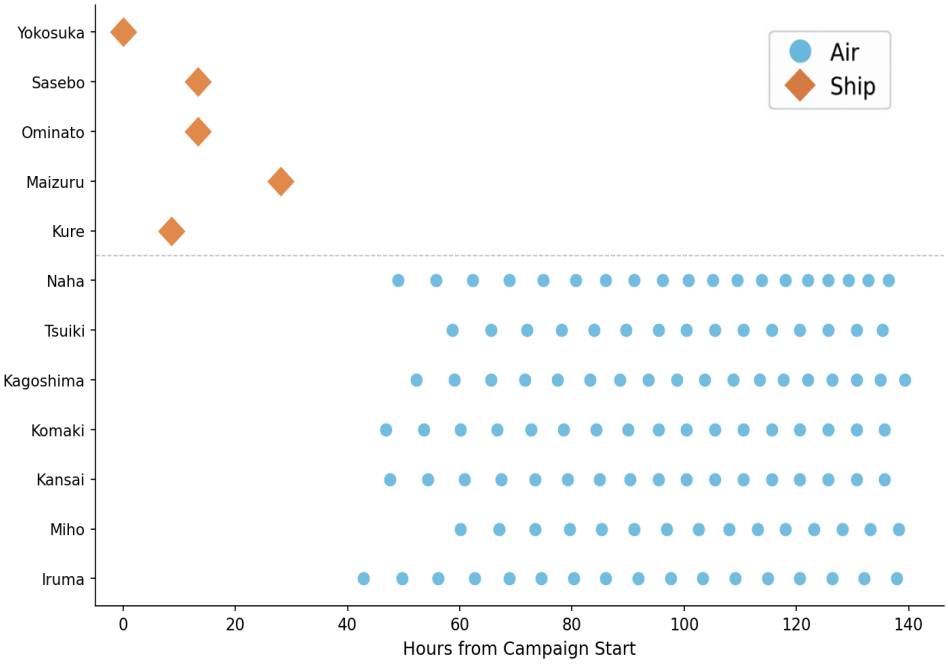


Figure 8 - Mode 4 delivery event timeline (Typhoon Meari (2004)). Each dot = one delivery sortie. Maritime ships (bottom) conduct a single delivery operation early in the campaign; existing airfields (top 7) cluster similarly; assumed island locations (middle 2, shaded) extend the campaign window substantially earlier.

Figure 9 quantifies total delivery sorties and total packages by airfield for both typhoon cases. For Typhoon Meari (2004), total sorties range from 15 (Miho, Tsuiki) to 19 (Naha), a spread of only 21% versus the 56% spread observed in Mode 1. The total packages delivered (60–76 packages for existing airfields) follow the same pattern. This compression of geographic sensitivity confirms the fundamental advantage of high-speed platforms: at 890 km/h cruise, the travel time penalty of a more distant airfield is absorbed within a single sortie window.

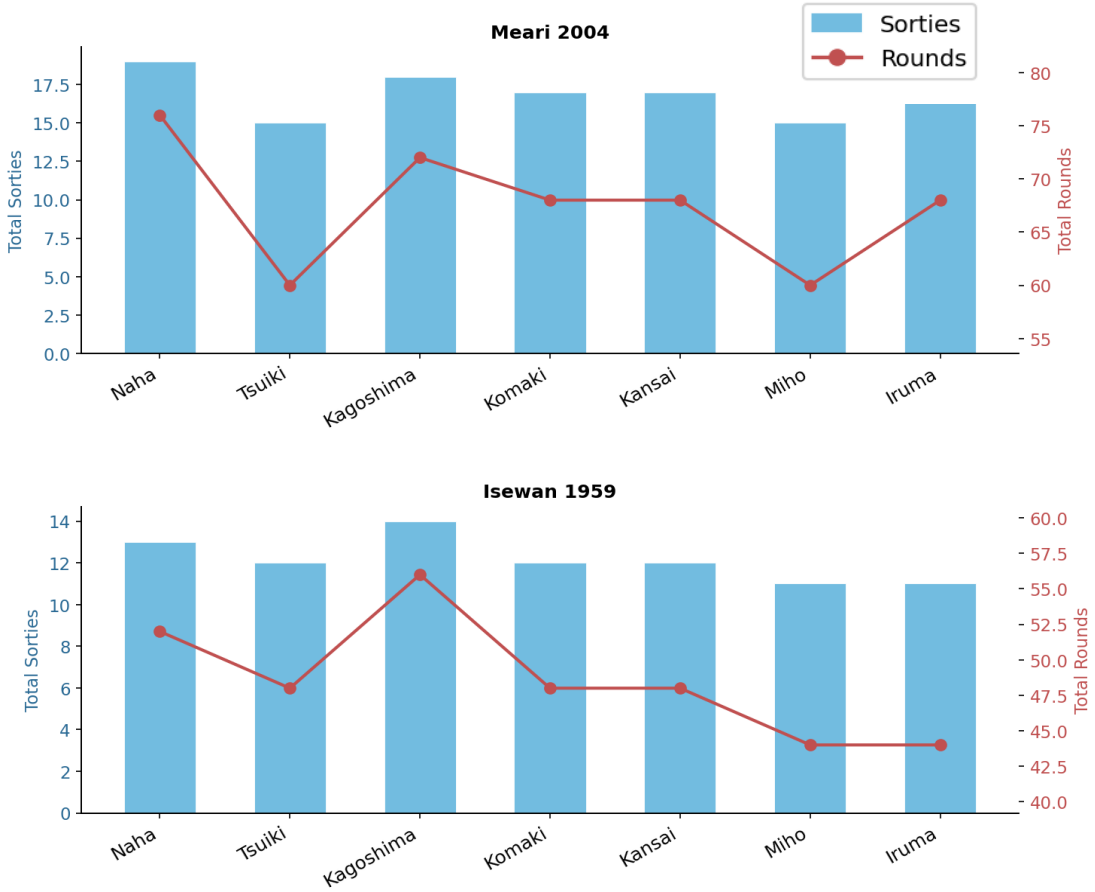


Figure 9 - Mode 4 aerial delivery: total sorties (bars) and total packages (secondary axis) by departure airfield for Typhoon Meari (2004) (left) and Typhoon Vera (1959) (right).

Table 5 provides a detailed Mode 4 summary. For Typhoon Meari (2004), the average inter-event interval (IEI)—the time between consecutive delivery sorties—is remarkably consistent at 4.9-5.9 hours across all existing airfields. This consistency reveals that the limiting factor for high-speed platforms is not geographic position but rather the typhoon's geometry: the radius of the delivery zone, the approach speed of the platform, and the turnaround cycle all determine the IEI, while airfield distance (within the range budget) affects only the available campaign window.

Table 5 - Mode 4 aerial delivery summary. IEI = inter-event interval (average time between sorties). Campaign = total operation window duration (Typhoon Meari (2004)).

Airfield	Meari (2004) Sorties	Meari (2004) Packages	Avg IEI (h)	Meari (2004) Campaign (h)	Vera (1959) Sorties	Vera (1959) Packages
Iruma	17	68	5.9	95.0	11	44
Komaki	17	68	5.6	88.9	12	48
Kansai	17	68	5.5	88.2	12	48
Miho	15	60	5.6	78.1	11	44
Tsuiki	15	60	5.5	76.7	12	48
Kagoshima	18	72	5.1	87.1	14	56
Naha	19	76	4.9	87.5	13	52

Figure 10 shows the campaign window duration and average IEI across all locations including the assumed island locations. The campaign window for existing airfields ranges from 76.7 h (Tsuiki) to 95.0 h (Iruma) for Typhoon Meari (2004)—a modest 24% spread. However, the assumed Minamitorishima scenario achieves a 207-hour window (8.6 days), compared to 87-95 hours for existing airfields. This dramatic extension arises because Minamitorishima can begin operations on the typhoon while it is still in the eastern Pacific on 08/26, whereas all existing airfields do not activate until 08/31—a full five days later. Despite this extended window, the average IEI for Minamitorishima (5.2 h) is similar to existing airfields, confirming that the typhoon's own geometry—not the airfield's location—governs sortie tempo.

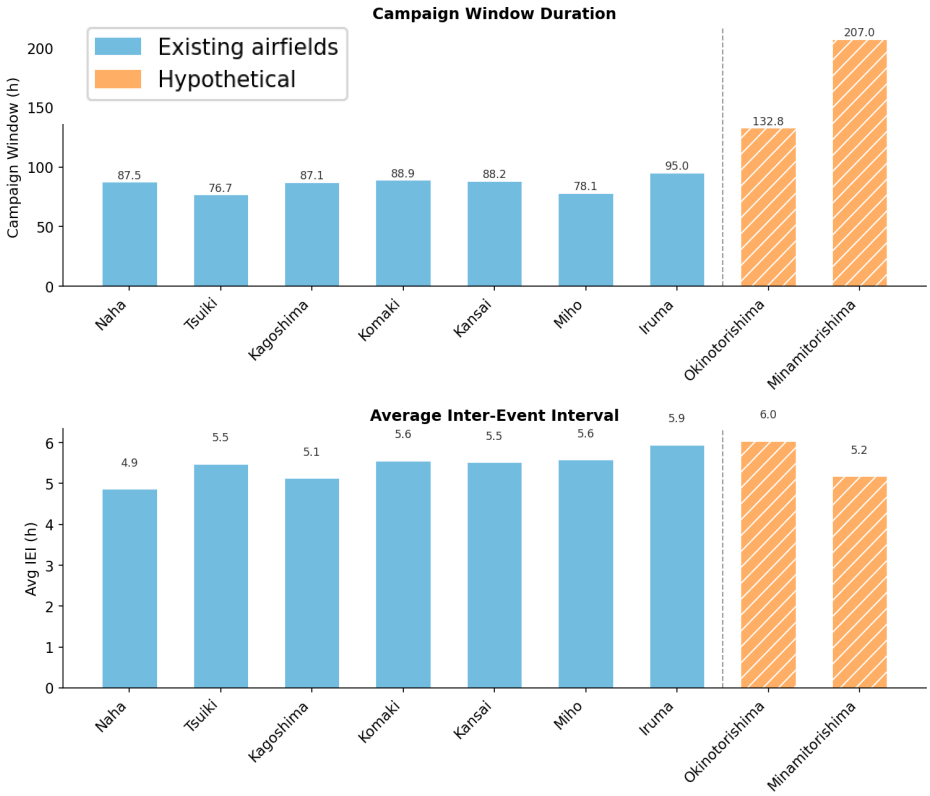


Figure 10 - Mode 4 campaign window duration (left) and average inter-event interval (right) by departure location (Typhoon Meari (2004)).

3.4.2 Mode 4 — Maritime Surface Platform Results

Three maritime surface platforms were modeled, each departing from different home ports along the Japanese coast. Each vessel achieved only a single delivery operation over the entire Typhoon Meari (2004) campaign, all occurring on 08/30—before the aerial platform campaigns begin on 08/31. At first glance, this single-event limitation might appear to make maritime platforms irrelevant. However, two features of these results are noteworthy.

First, the timing of the maritime delivery operation (08/30) is actually earlier than any aerial platform's first sortie. This reflects an important structural difference: maritime platforms, despite their slow speed, are already deployed at sea and do not require an airfield infrastructure. They can position themselves during the typhoon's Pacific approach and operate at maximum range on their first opportunity. The single delivery operation yields 8 delivered packages—twice the four packages delivered per aerial sortie—and occurs at a stage of the typhoon's lifecycle when it is still over deep ocean and potentially most susceptible to modification.

Second, the single-operation limitation is a direct consequence of the vessel's inability to reposition quickly enough to conduct a second delivery operation before the typhoon accelerates toward landfall. As discussed in Section 4.3, this limitation is geometric rather than fundamental: a pre-positioned

vessel in the western Pacific can achieve three to five delivery operations. The maritime platform therefore represents a complementary capability—an early-campaign delivery layer—rather than a replacement for the sustained aerial delivery provided by transport aircraft in Modes 1-3.

4. Discussion

4.1 Track Alignment as the Primary Operational Parameter

The reversal in optimal airfield between Typhoon Meari (2004) (Naha optimal, 70 sorties) and Typhoon Vera (1959) (Kagoshima optimal, 46 sorties) persists consistently across Modes 1 through 4. The mechanism is geometric: the airfield that lies ahead of the typhoon's approach corridor benefits from earlier campaign activation and a longer window before the strong wind zone terminates operations. The practical implication is that typhoon control logistics cannot rely on a static designated hub; the active hub must be reassigned dynamically as 48–72-hour track forecasts are updated.

4.2 High-Speed Platforms: Campaign Window vs. Sortie Frequency

A key insight from Mode 4 is that geographic distance has a qualitatively different effect on high-speed platforms than on transport aircraft. For transport aircraft (Modes 1-3), a more distant airfield directly reduces sortie count by increasing round-trip time. For high-speed delivery platforms (Mode 4), the inter-event interval (IEI) is governed primarily by the typhoon's geometry—delivery zone radius, platform approach speed, and turnaround cycle—yielding a near-constant IEI of approximately 5.0-5.9 hours across all existing airfields regardless of distance.

What distance does affect for high-speed platforms is the available campaign window: a distant airfield activates later because the typhoon must travel closer before it enters the platform's range. This effect is small for existing airfields (76–95-hour window range) but becomes dramatic for the assumed Minamitorishima scenario, where the 207-hour window enables 41 delivery sorties compared to 15-19 from existing locations. For operational planning purposes, this means the priority for high-speed platform deployment is not proximity perse but ensuring campaign activation at the earliest possible typhoon phase.

4.3 Maritime Platforms as an Early-Campaign Complementary Layer

The simulation reveals a natural temporal complementarity between maritime platforms and aerial platforms. Maritime vessels engage the typhoon on 08/30—approximately 24 hours before the aerial campaign begins—providing an early-campaign delivery capability that aerial platforms from existing airfields cannot match. At this early stage, the typhoon is over deep ocean at lower intensity; the ability to deliver influence substances before the typhoon reaches peak intensity may be of particular value from a meteorological modification standpoint.

The per-operation delivery capacity of maritime platforms (8 packages) exceeds the per-sortie capacity of aerial platforms (4 packages), making each maritime delivery operation equivalent to two aerial sorties in terms of delivered material. The strategic implication is that maritime and aerial platforms should be viewed as complementary rather than competitive: maritime platforms provide high-payload early-campaign delivery, while aerial platforms provide sustained tempo throughout the campaign's middle and final phases.

The limitation—one delivery operation from home ports—is addressed by pre-positioning in the western Pacific forward zone (145–155°E for Meari-type tracks), enabling three to five maritime delivery operations distributed across the campaign's timeline rather than concentrated at a single early point. This temporal distribution of maritime deliveries would provide more sustained early-phase support and potentially allow iterative assessment of atmospheric modification effects before the peak aerial campaign phase.

4.4 Non-linear Range Threshold Effects

Turboprop platforms exhibit a distinctive cliff-edge behavior: the Q400AT qualifies for single-lap missions only from Naha andbecomes completely infeasible from all airfields in three-lap modes—without intermediate degradation. This binary behavior arises because the sum of transit distance plus on-station fuel consumption either fits within or exceeds the range budget. Operational planning must maintain continuously updated range-feasibility maps for each airfield-aircraft combination as the typhoon approaches.

4.5 Integrated System Architecture

Synthesizing the Mode 1-4 results, an optimal typhoon control delivery system architecture comprises four integrated components. First, a dynamically selected hub airfield (updated every 24–48 hours based on track forecasts) provides the logistics backbone for bulk transport operations in Modes 1-3. Second, the C-2 Long-Range variant serves as the universal transport backbone, viable from all airfields for all mission profiles. Third, turboprop and civil aviation assets (C-130H, Q400AT) contribute a proximity bonus when within their range envelope, supplementing the high-capacity C-2 at closer hubs. Fourth, Mode 4 operations are structured in two temporal layers: maritime platforms provide high-payload early-campaign delivery during the typhoon's open-ocean phase, while high-speed aerial platforms from airfields sustain delivery tempo throughout the approach phase. The MQ-9 UAV operates continuously as a real-time monitoring and precision delivery platform independent of the logistics hub.

5. Geographic Sensitivity Analysis: Actual Remote Japanese Pacific Island Locations

Having established that geographic alignment governs operational performance across all four modes, this section quantifies the theoretical upper bound by testing two actual Japanese remote Pacific island locations—Minamitorishima (24.3°N, 153.97°E) and Okinotorishima (20.4°N, 136.1°E)—under the assumption that airfields with takeoff and landing capability are available at each location. Neither island currently possesses such infrastructure; this analysis is a purely academic parametric sensitivity study and does not constitute or advocate any infrastructure recommendation.

5.1 Setup and Scope

These assumed island locations were tested under the Typhoon Meari (2004) case using the same parameters as the main analysis. The Typhoon Vera (1959) case was not run for these locations as its track geometry does not traverse the Pacific corridor where Minamitorishima's advantage manifests.

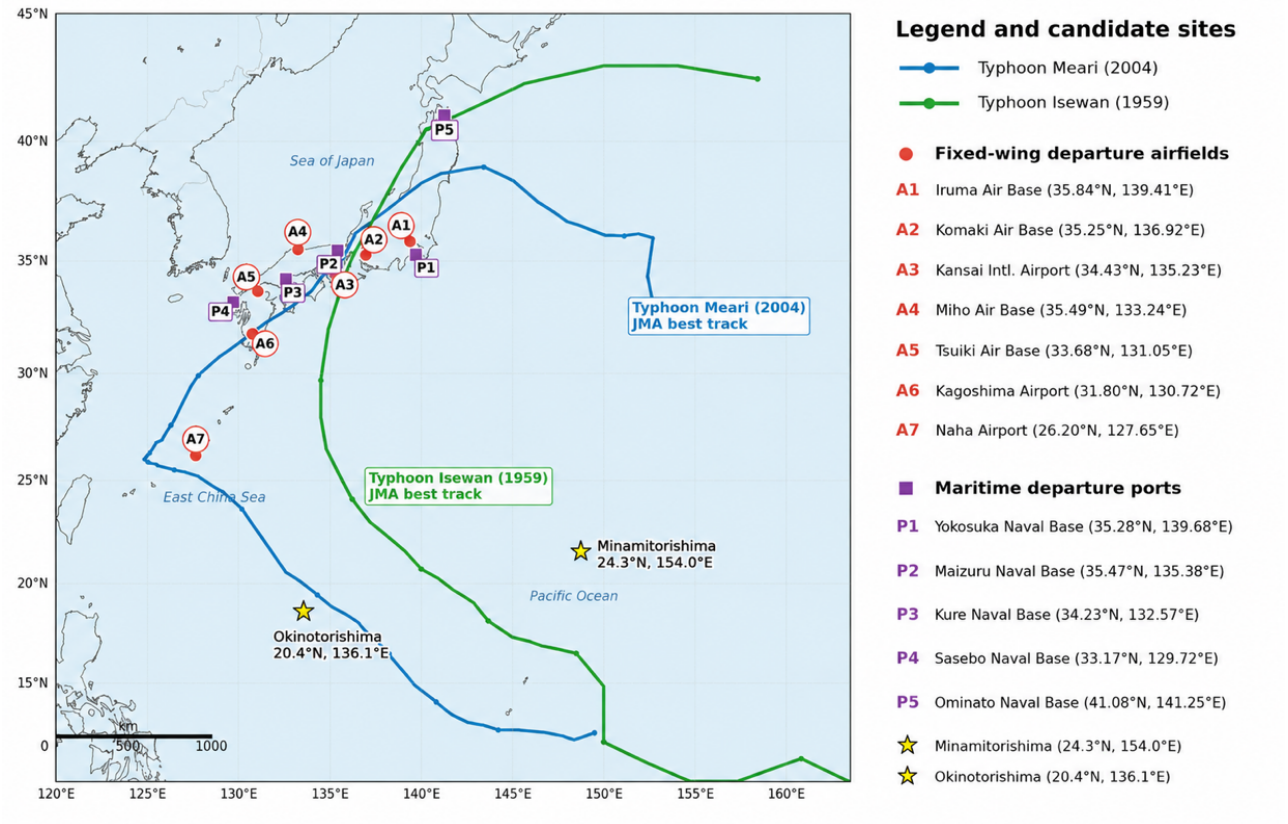


Figure 11 - Geographic context of assumed island locations relative to the Typhoon Meari (2004) typhoon track.

Table 6 - Assumed island locations for geographic sensitivity analysis.

Assumed Island Location	Coordinates	Dist. to Meari (2004) Track
Minamitorishima	24.3°N, 154.0°E	~200 km (early phase)
Okinotorishima	20.4°N, 136.1°E	~700 km (early phase)

5.2 Mode 1 and Mode 3 Results

Figures 12 and 13 present comparative Mode 1 and Mode 3 results for all nine locations. Minamitorishima achieves 127 total sorties and 2,664 t transport volume—81% more sorties and 85% more volume than Naha. In Mode 3, C-2 Long-Range averages 6.8 laps per sortie from Minamitorishima versus 5.1 from Naha, and the MQ-9 achieves 6.2 laps (versus 3.9 from Naha). Okinotorishima achieves 66 sorties and 1,377 t—comparable to Naha—reflecting its less favorable longitudinal alignment.

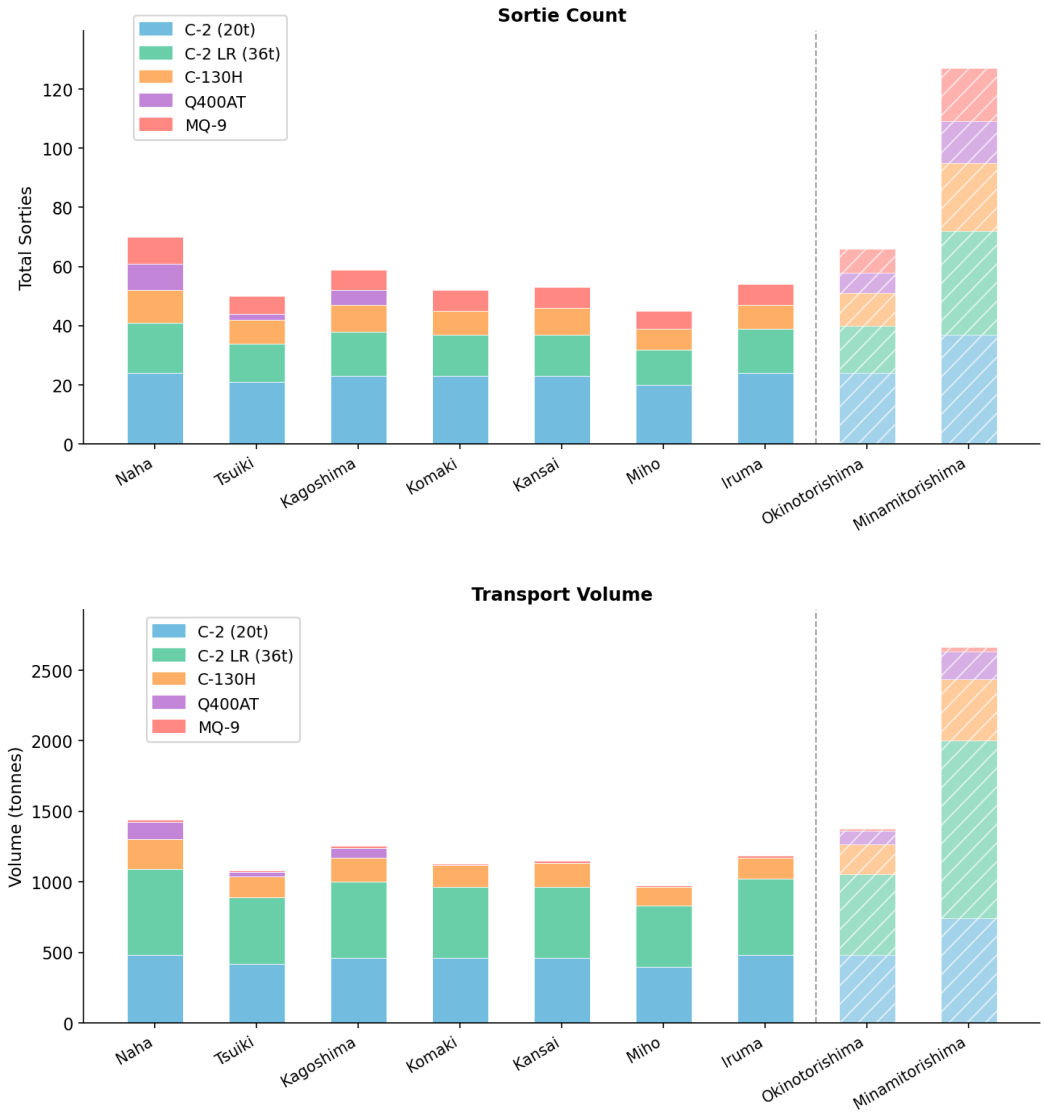


Figure 12 - Sensitivity analysis: Mode 1 sortie count (top) and volume (bottom) for all 9 locations (Typhoon Meari (2004)). Shaded = assumed.

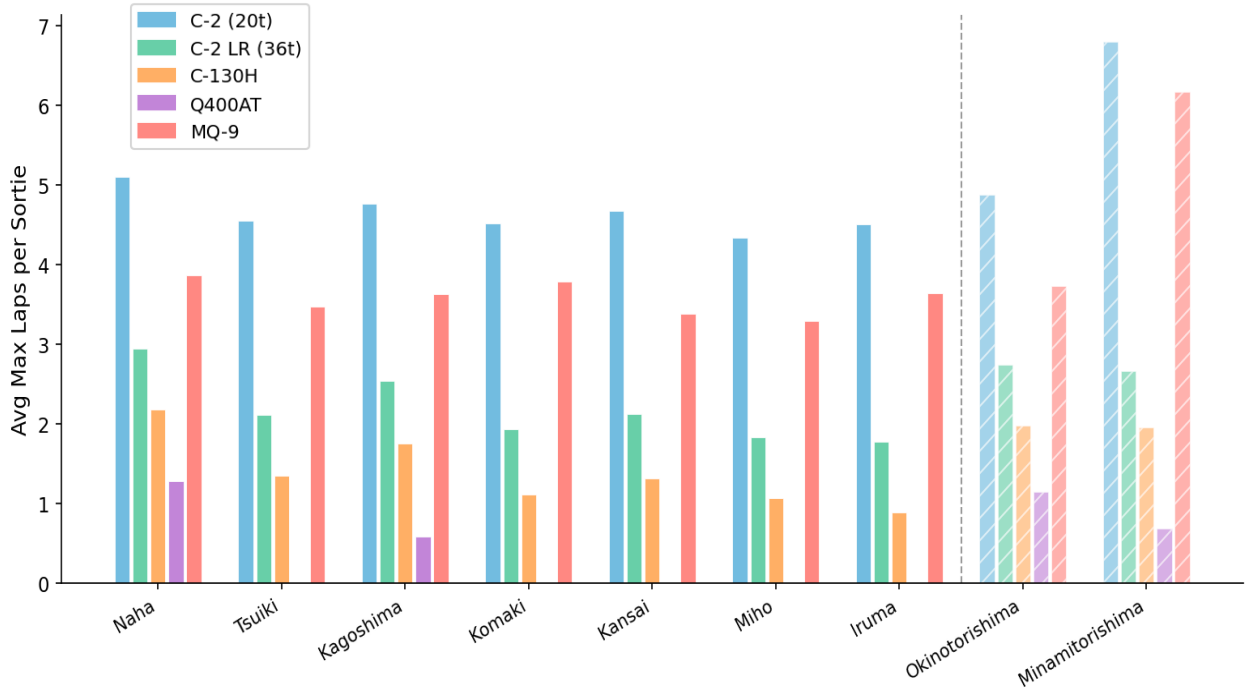


Figure 13 - Sensitivity analysis: Mode 3 average maximum laps (Typhoon Meari (2004)). Shaded = assumed.

5.3 Mode 4 Results for Assumed Island Locations

The Mode 4 timeline in Figure 8 shows the most dramatic manifestation of the geographic effect for high-speed platforms. Minamitorishima's aerial delivery campaign spans 207 hours (41 sorties, 164 packages), starting on 08/26—five days before any existing airfield can begin operations. This extended window is the pure geometric consequence of Minamitorishima's 153.97°E position: the Meari track passes within range of this location while the storm is still in the central Pacific, a phase that is geometrically inaccessible to all existing Japanese airfields.

Critically, the average IEI from Minamitorishima (5.2 h) is nearly identical to that of existing airfields (4.9–5.9 h), confirming that the sortie frequency advantage is entirely due to the longer campaign window, not faster platform tempo. For every additional day of campaign window, approximately four to five additional delivery sorties are achievable, independent of airfield location.

5.4 Implications for Logistics Architecture

These results establish three design principles. First, geographic positioning of the departure node relative to the typhoon's early-approach corridor is the dominant design parameter across all platform types. Second, for high-speed delivery platforms, the priority is maximizing the campaign window by early activation, not minimizing airfield-to-typhoon distance per se. Third, the performance gap between existing infrastructure and the theoretical optimum (81% sortie increase from Minamitorishima) provides a clear target for intermediate logistics concepts—advance maritime pre-positioning, aerial refueling relays, or cooperative Pacific staging—that could partially capture the geographic advantage without requiring permanent remote-island infrastructure.

6. Conclusion

This study evaluated typhoon control delivery feasibility through a four-mode simulation framework. The principal conclusions are:

- Track alignment governs operational throughput across all modes. Naha is optimal for Meari-type recurving typhoons; Kagoshima for Vera-type direct tracks. Dynamic hub selection based on 48–72-hour forecasts is essential.
- For transport aircraft (Modes 1-3), geographic distance directly limits sortie count through round-trip time. The non-linear range cliff of turboprops requires continuously updated range-feasibility monitoring.
- For high-speed delivery platforms (Mode 4), the campaign window—not sortie frequency—is the key geographic variable. The average inter-event interval of ~5 hours is nearly constant across all airfield locations; additional campaign time directly translates to approximately four to five additional delivery sorties per day.
- Maritime platforms provide an early-campaign complementary capability, initiating delivery approximately 24 hours before aerial platforms activate and delivering 8 packages per delivery operation (twice the aerial rate). Pre-positioning in the western Pacific (145–155°E for Meari-type) extends this to three to five delivery operations distributed across the campaign timeline.
- The geographic sensitivity analysis (Section 5) shows that an assumed departure point at Minamitorishima (153.97°E) would yield 81% more sorties, 85% more transport volume, and a 5-day earlier campaign activation for Meari-type recurving typhoons—entirely due to geometric advantage. This provides a theoretical benchmark for evaluating intermediate forward-staging logistics concepts.

Future work will extend the framework to: probabilistic analysis over multi-decade typhoon track databases; resource-constrained fleet optimization with finite influence substance stockpiles; meteorological constraints on operations in the typhoon rainband; evaluation of intermediate forward

staging concepts (aerial refueling, maritime pre-positioning logistics); and sensitivity analysis on R15 model parameters. The long-term objective is an integrated end-to-end mission planning framework supporting both pre-mission design and real-time operational decisions for typhoon control campaigns.

7. Acknowledgements

The author thanks the members of the Institute for Multidisciplinary Sciences at Yokohama National University for valuable feedback. This research was supported by the Moonshot Research and Development Program by Japan Science and Technology Agency (JST) [grant number JPMJMS2282]. Historical typhoon best-track data were obtained from the Japan Meteorological Agency.

8. Copyright Statement

The authors confirm that they, and/or their company or organization, hold copyright on all of the original material included in this paper. The authors also confirm that they have obtained permission, from the copyright holder of any third-party material included in this paper, to publish it as part of their paper. The authors confirm that they give permission or have obtained permission from the copyright holder of this paper, for the publication and distribution of this paper as part of the ICAS proceedings or as individual off-prints from the proceedings.

9. References

[1] Cabinet Office. "Moonshot Goal 8." Japan Science and Technology Agency, 2021.

[2] Kawasaki Heavy Industries. C-2 Transport Aircraft Product Overview. Kawasaki Technical Review No. 179, 2018.

[3] U.S. Air Force. C-130 Hercules Fact Sheet. U.S. Air Force, 2023.

[4] De Havilland Aircraft of Canada Ltd. Dash 8-400 Specifications Sheet. De Havilland, 2025.

[5] U.S. Department of Defense. MQ-9 Reaper Armed UAS. FY2017 Annual Report, 2017.

[6] Dantzig, G.B. and Ramser, J.H. "The Truck Dispatching Problem." Management Science, 6(1), 80-91, 1959.

[7] Toth, P. and Vigo, D. (eds.). The Vehicle Routing Problem. SIAM Monographs on Discrete Mathematics and Applications, Philadelphia, 2002.

[8] Golden, B.L., Raghavan, S. and Wasil, E.A. (eds.). The Vehicle Routing Problem: Latest Advances and New Challenges. Springer, New York, 2008.

[9] Savelsbergh, M.W.P. and Sol, M. "The General Pickup and Delivery Problem." Transportation Science, 29(1), 17-29, 1995.

[10] Laporte, G. "The Vehicle Routing Problem: An Overview of Exact and Approximate Algorithms." European Journal of Operational Research, 59(3), 345-358, 1992.